JOURNAL OF GUIDANCE, CONTROL, AND DYNAMICS
Vol. 23, No. 2, March–April 2000

Simple Analytic Model of the Long-Term Evolution of Nanosatellite Constellations

Colin R. McInnes*
University of Glasgow, Glasgow, Scotland G12 8QQ, United Kingdom

The long-term evolution of a large constellation of nanosatellites is investigated using closed-form analytical methods. A set of partial differential equations is derived, the solution to which provides the evolution of the mean spatial number density of the constellation under the action of air drag, on-orbit satellite failures, and the deposition of new satellites into the constellation. These solutions give insight into the global dynamics and long-term evolution of large constellations of nanosatellites and display some interesting physical features. In particular, asymptotic solutions provided the steady-state distribution of nanosatellites and an estimate of the required rate of deposition of new nanosatellites to maintain the constellation.

Nomenclature

a = drag-induced acceleration
B = ballistic coefficient
H = atmospheric scale height
n = number density
R = reference radius
r = radial coordinate
z = out-of-plane coordinate
η = mean failure rate
θ = azimuthal coordinate
μ = gravitational parameter
ρ = air density
ρ_0 = base density at radius R
ω = orbital angular velocity

I. Introduction

NANOSATELLITES are seen as a low-cost means of enabling a diverse range of innovative new mission applications.[1] Developments in miniaturization using microelectromechanical systems (MEMS) technology leads to projected nanosatellite masses of less than 1 kg. In some instances, simple satellites-on-a-chipmay have a mass of order 10^{-3} kg (sometimes termed picosatellites).[2,3] A particularly attractive concept is the use of large numbers of such nanosatellites (or picosatellites) to form constellations to allow the real-time acquisition of distributed information. For example, a spherical constellation of nanosatellites has been proposed to provide a real-time, three-dimensional view of the magnetosphere.[4] Each nanosatellite can be thought of as a pixel (a so-called pixie) of a three-dimensional data set. To provide good spatial and temporal resolution for such a mission, large numbers of nanosatellites are required. For MEMS fabricated nanosatellites, with a mass of order 0.1 kg or less, constellations may contain several thousand members. Because these ultralow mass satellites may be passive sensors without active orbit control, environmental effects such as air drag will shape the evolution of the constellation.

Other concepts have envisaged large numbers ($>10^3$) of nanosatellites to be deployed from a dispenser to provide a continuous planar ring of satellites for communication purposes.[5] Such constellations would be formed by dispensing nanosatellites over a range of orbit radii at the same inclination to induce differential azimuthal motion, thus forming a uniform ring. With a large number of satellites in essentially random azimuthal locations, communication links become robust to on-orbit failures. Furthermore, the constellation is only short-lived because air drag will eventually remove all of the nanosatellites. Such concepts are attractive for military communications, where the constellation is deployed from a single launch vehicle and formed to support a dedicated remote operation. A related concept requires clusters of nanosatellites to be launched into random orbits to provide a uniform spherical constellation, possibly as piggyback launches on any available vehicle.[6] Analysis shows that 400 nanosatellites can provide ~95% coverage of the globe. The constellation would require the continual deposition of new nanosatellites to make up for losses from on-orbit failures and air drag removal.

Whereas such missions will provide new opportunities for space science and communications, they also pose interesting new problems in orbital dynamics. Because of their low mass and cross section, nanosatellites will have a ballistic coefficient that is significantly different from conventional satellites.[3] For a satellite of characteristic dimension l, its mass will scale as l^3, whereas its crossection will scale as l^2. As the satellite shrinks in physical size, its area-to-mass ratio will, therefore, increase as l^{-1} so that air drag, and, in high orbits, light pressure, will provide major perturbations. In addition, because of the large number of nanosatellites that may be used to form a single mission constellation, the population dynamics of the constellation becomes important. Once the constellation is formed, differential air drag will induce shearing motion on the radial distribution of nanosatellites and, in the absence of active orbit control, will remove those members of the constellation at low altitudes. Similarly, random on-orbit failures will deplete the constellation while the launch and deposition of new nanosatellites will replenish the constellation.

In this paper the evolution of constellations of large numbers of nanosatellites will be investigated. It will be assumed that the nanosatellites form either a uniform planar ring constellation, or a uniform spherical constellation, as discussed earlier. Therefore, the constellation will be characterized by the mean spatial number density of nanosatellites as a function of both orbit radius and time. Using approaches developed for studies of orbit debris evolution,[7] partial differential equations will be derived that describe the temporal and spatial evolution of some initial distribution of nanosatellites. These equations are essentially continuity equations that represent the effect of differential air drag on the radial distribution of nanosatellites, random on-orbit failures, and the deposition of new nanosatellites to replenish and maintain the constellation. Analytical solutions to the continuity equations will be obtained using the method of characteristics. These solutions then illustrate the effect of various processes on the evolution of the constellation. The long-term, asymptotic distribution of nanosatellites is also obtained, and an inverse problem posed. The inverse problem provides the required mean deposition rate of new nanosatellites to maintain some required steady-state constellation. Although the modeling of the dynamics of the constellation is relatively simple, the analysis provides analytic solutions, and therefore insight, into the long-term population dynamics of nanosatellite constellations.

Received 19 February 1999; revision received 15 July 1999; accepted for publication 13 August 1999.

*Professor, Department of Aerospace Engineering; colinmc@aero.gla.ac.uk.

II. Constellation Formation

Before investigating the evolution of nanosatellite constellations, their formation will briefly be investigated. Dispersal methods for conventional, actively controlled constellations are well established whereby a dispenser is used to maneuver and place each satellite at an appropriate azimuthal position. Because of the large energy costs associated with significant plane changes, each dispenser will typically form only a single plane of the constellation. For a nanosatellite constellation, careful azimuthal positioning of each satellite is unimportant because large numbers of uncontrolled nanosatellites provide a mean, uniform distribution. In this case, differential azimuthal motion due to differences in orbit radius will provide a uniform distribution of nanosatellites. Typically, the dispenser will inject nanosatellites into the constellation over a range of orbit radii to provide such differential azimuthal motion, as discussed in Sec. I. By the use of a range of orbit planes and differential nodal drift, a spherical constellation can also be formed, as shown in Fig. 1.

The timescale required to obtain a uniform azimuthal distribution of nanosatellites can be estimated from the differential azimuthal rates of the nanosatellites. For a circular orbit of radius r the orbital angular velocity is given by

$$\omega = \sqrt{\mu / r^3} \tag{1}$$

Therefore, the azimuthal rate of a nanosatellite on a neighboring circular orbit separated by Δr may be written as

$$\Delta\omega = \frac{\partial \omega}{\partial r}\Delta r \tag{2}$$

The time to obtain a uniform azimuthal distribution of nanosatellites can now be estimated from the time required for the leading nanosatellite at orbit radius r to complete one orbit relative to the trailing nanosatellite at orbit radius $r + \Delta r$. This is just the synodic period of the two satellites. Therefore, the time to obtain a uniform distribution T_θ is defined by $T_\theta|\Delta\omega| = 2\pi$ so that

$$T_\theta \sim (4\pi/3\sqrt{\mu})(r^{\frac{5}{2}}/\Delta r) \tag{3}$$

This timescale is shown in Fig. 2 for a range of orbit separations Δr. Even for a relatively narrow distribution of orbit radii, the timescale will be short relative to the timescale for orbit decay due to air drag. For a planar constellation it will, therefore, be assumed that the mean constellation number density is a function of orbit radius and time only.

To establish a spherical constellation of nanosatellites, a more complex dispersal strategy is required. For such a spherical distribution the nanosatellites must be dispersed with a uniform distribution in latitude that in fact requires a uniform ascending node distribution but a nonuniform inclination distribution. Whereas a uniform distribution in orbit azimuth can be obtained by exploiting differential azimuthal motion, a uniform distribution in an ascending node is more problematic. Differential nodal drift due to Earth oblatness is a candidate mechanism for dispersal; however, the differential rates are exceedingly slow. A truly uniform spherical constellation can then only be established by either a maneuvering dispenser or several launches. Because of the significant energy required to rotate the dispenser orbit plane, a single dispenser will only form part of the constellation. Launches of clusters of nanosatellites to various orbital planes will, therefore, be required to complete the formation of a spherical constellation. Alternatively piggyback launches of clusters of nanosatellites on any available vehicle may also be used to assemble a spherical constellation, as discussed in Sec. I.

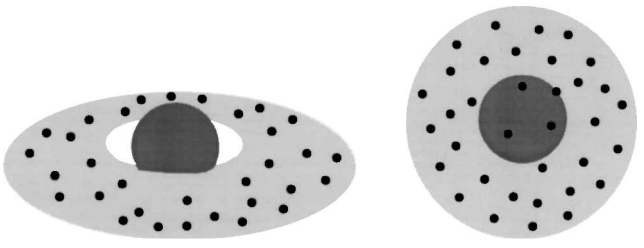

Fig. 1 Planar and spherical constellations of nanosatellites.

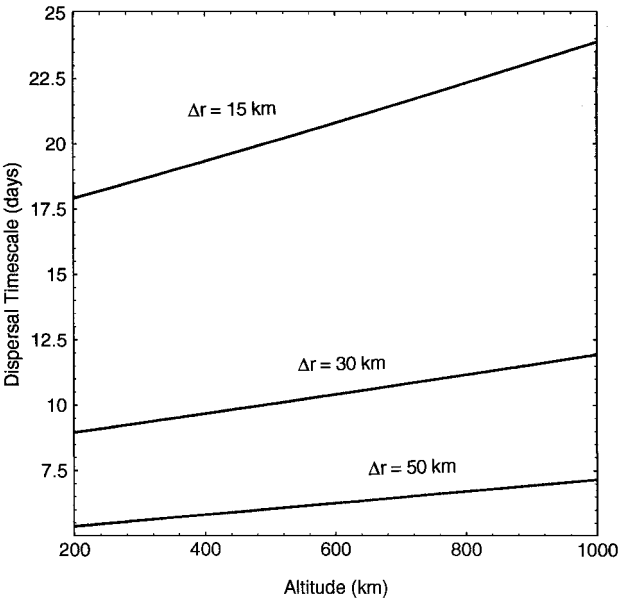

Fig. 2 Azimuthal dispersal timescale.

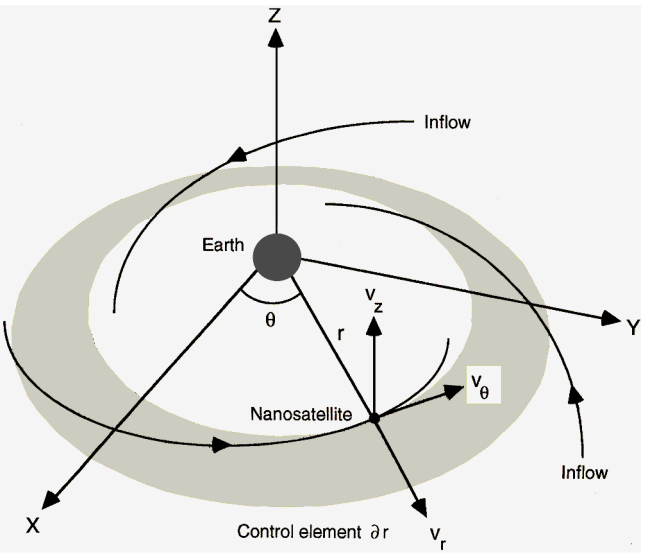

Fig. 3 Planar constellation dynamics.

III. Evolution Equation for a Planar Constellation

In this initial analysis, it will be assumed that the constellation of nanosatellites forms a planar, near equatorial disk. The disk will be formed through differential azimuthal motion, as described in Sec. II. The timescale for azimuthal dispersal T_θ will be assumed to be small relative to the timescale for evolution of the radial profile of the constellation under the action of air drag. An individual nanosatellite will be located within the constellation using cylindrical polar coordinates (r, θ, z), as shown in Fig. 3. The nanosatellite will then have a velocity vector (v_r, v_θ, v_z) where the z component of velocity will be assumed to be negligible due to the low inclination of the constellation disk. Under the slow action of air drag, the satellite transverse velocity will be near Keplerian so that

$$v_r = -f(r, B) \tag{4a}$$

$$v_\theta \sim \sqrt{\mu / r} \tag{4b}$$

$$v_z \sim 0 \tag{4c}$$

where the inward drift velocity v_r ($\ll v_\theta$) is a function of orbit radius and the nanosatellite ballistic coefficient B. Although this analysis will consider nanosatellites with a single ballistic coefficient, the evolution of a distribution of ballistic coefficients may be obtained by a superposition of mean spatial number density solutions.

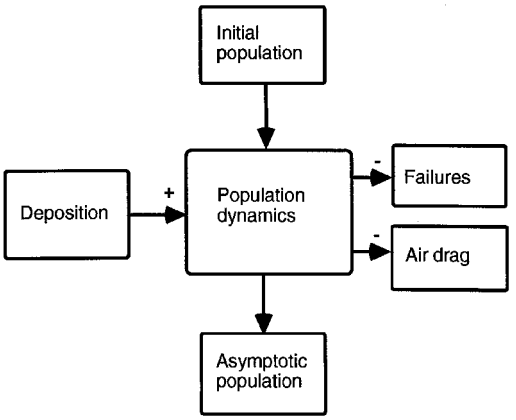

Fig. 4 Constellation population dynamics.

Because the inward drift velocity is a function of altitude only, the nanosatellite radial density distribution will be sheared due to differential air drag. An initial disk that is radially compact soon after formation will diffuse downward and will be sheared into a more extended form.

If the nanosatellites are assumed to be distributed uniformly in azimuth on a near equatorial disk, the constellation may be characterized by a mean spatial number density $n(r, t)$. An annulus of the constellation bounded by ∂r in the interval $[r, r + \Delta r]$ will contain $2\pi r \Delta r n(r, t)$ nanosatellites, as shown in Fig. 3. Therefore, the rate of change of the number of nanosatellites is obtained by considering the flow to and from this control volume from neighboring annuli, while allowing for the addition and removal of nanosatellites, namely,

$$\frac{\partial}{\partial t}[2\pi r \Delta r n(r, t)] = 2\pi r v_r(r) n(r, t) - 2\pi(r + \Delta r) v_r(r + \Delta r) \times n(r + \Delta r, t) + 2\pi r \Delta r[\dot{n}^+(r) - \dot{n}^-(r)] \tag{5}$$

The deposition of new nanosatellites is described by $\dot{n}^+(r, t)$, whereas the failure of existing nanosatellites is described by $\dot{n}^-(r, t)$. This process is shown schematically in Fig. 4. The radial drift rate and density function may now be expanded to first order. Then, taking the limit $\Delta r \to 0$ it is found that

$$\frac{\partial n(r, t)}{\partial t} + \frac{1}{r}\frac{\partial}{\partial r}[r v_r(r) n(r, t)] = \dot{n}^+(r) - \dot{n}^-(r) \tag{6}$$

which is a continuity equation for the mean number density of nanosatellites. It is this partial differential equation that describes the evolution of the nanosatellite constellation as a function of both orbit radius and time. Differentiating the second term and recognizing that v_r is a function of altitude only, Eq. (6) may be written as

$$\frac{\partial n(r, t)}{\partial t} + \frac{\partial n(r, t)}{\partial r} v_r(r) + n(r, t)\left[\frac{v_r'(r)}{v_r(r)} + \frac{1}{r}\right] v_r(r) = \dot{n}^+(r) - \dot{n}^-(r) \tag{7}$$

where the prime represents a differentiation with respect to r. This linear partial differential equation may now be solved using the method of characteristics (for example, see Ref. 8). In particular, the solution to Eq. (7) is obtained from the identity

$$\left[-n(r, t)\left[\frac{v_r'(r)}{v_r(r)} + \frac{1}{r}\right] v_r(r) + \dot{n}^+(r) - \dot{n}^-(r)\right]^{-1} \mathrm{d}n = v_r(r)^{-1}\,\mathrm{d}r = \mathrm{d}t \tag{8}$$

which provides two ordinary differential equations, namely,

$$\frac{\mathrm{d}r}{\mathrm{d}t} = v_r(r) \tag{9a}$$

$$\frac{\mathrm{d}n(r, t)}{\mathrm{d}r} + n(r, t)\left[\frac{v_r'(r)}{v_r(r)} + \frac{1}{r}\right] = \frac{1}{v_r(r)}[\dot{n}^+(r) - \dot{n}^-(r)] \tag{9b}$$

Equation (9a) represents the family of characteristics of the partial differential equation. It can be seen that the characteristics are defined by the inward spiral trajectories of the nanosatellites. After solving Eq. (9a) to obtain the characteristics, the evolution equation [Eq. (9b)] may be solved to obtain the expected number density of nanosatellites under the action of air drag and various models for the forcing terms $\dot{n}^+(r)$ and $\dot{n}^-(r)$. As will be seen, the solution of the partial differential equation will require some initial data $n(r, 0)$, representing the initial distribution of nanosatellites. This is the so-called Cauchy boundary value problem for the partial differential equation.

IV. Solution of the Characteristic Equation

To integrate Eq. (9a), it is necessary to obtain the radial drift velocity v_r due to air drag. This drift velocity may be obtained from the rate of loss of energy due to the nonconservative drag acceleration. The drag acceleration exerted on a nanosatellite of ballistic coefficient B is modeled in this study as

$$a = \tfrac{1}{2}B^{-1}\rho(r)v^2, \qquad \rho(r) = \rho_0 \exp[-(r - R)/H] \tag{10}$$

where the air density $\rho(r)$ is modeled by a single exponential function with scale height H and base density ρ_0 at some reference radius R. A scale height of 60 km is used with a base density of 5×10^{-9} kg $\cdot$ m^{-3} at reference altitude of 200 km ($R = 6571$ km). This provides an approximate fit to the observed air density profile.[9] Because of rapid orbit decay below 200 km, nanosatellites below this altitude are considered to be lost from the constellation. For a nanosatellite of mass m, cross section A, and drag coefficient C_D, the ballistic coefficient is $m/C_D A$. The nanosatellite ballistic coefficient is chosen to be 20 kg $\cdot$ m^{-2}, representative of a 0.1-kg, 5-cm cubic nanosatellite with a body density of 800 kg $\cdot$ m^{-3}. A pure silicon nanosatellite would have a body density of 2.3×10^3 kg $\cdot$ m^{-3}. Because the drag acceleration acts opposite to the nanosatellite velocity vector, the rate of loss of energy E of the satellite is then given by $\mathrm{d}E/\mathrm{d}t = -v_\theta a$. Furthermore, for a near circular orbit of radius r, the instantaneous energy $E = -\mu/2r$. Then, using the approximation $v_\theta \sim \sqrt{(\mu/r)}$, the radial drift velocity may be written as

$$v_r(r) \sim -\sqrt{\mu r}\,B^{-1}\rho_0 \exp[-(r - R)/H] \tag{11}$$

so that the characteristic equation is now obtained from

$$\int \frac{\exp[r/H]}{\sqrt{r}}\,\mathrm{d}r + \varepsilon t = C, \qquad \varepsilon = \sqrt{\mu}B^{-1}\rho_0 \exp\left[\frac{R}{H}\right] \tag{12}$$

where C is a constant of integration. This integration may be easily performed if the approximation is made that $\sqrt{r} \sim \sqrt{R}$. In the context of Eq. (12), this requires that the change in nanosatellite velocity is ignored relative to the change in air density, which is accurate to order 10^{-2} for altitudes below 10^3 km (Ref. 9). If this approximation is not made Eq. (12) may still be integrated, although the solution is obtained in terms of the error function erf(r). The characteristics of the partial differential equation are now given by

$$\exp[r/H] + (\varepsilon\sqrt{R}/H)t = \tilde{C}, \qquad \tilde{C} = -(\varepsilon\sqrt{R}/H)C \tag{13}$$

which may be written as $G(r, t) = \tilde{C}$. The family of characteristics shown in Fig. 5 clearly demonstrates the significant air drag experienced by nanosatellites and the shearing effect due to differential air drag. It is this shearing motion that will have a major influence on the long-term dynamics of the nanosatellite constellation.

V. Solution of the Evolution Equation for a Planar Constellation

Having obtained the characteristics of the partial differential equation, the evolution equation [Eq. (9b)] can now be solved using standard solution methods for ordinary differential equations. For illustration, the forcing terms $\dot{n}^+(r, t)$ and $\dot{n}^-(r, t)$ will first be removed so that the solution describes the evolution of some initial

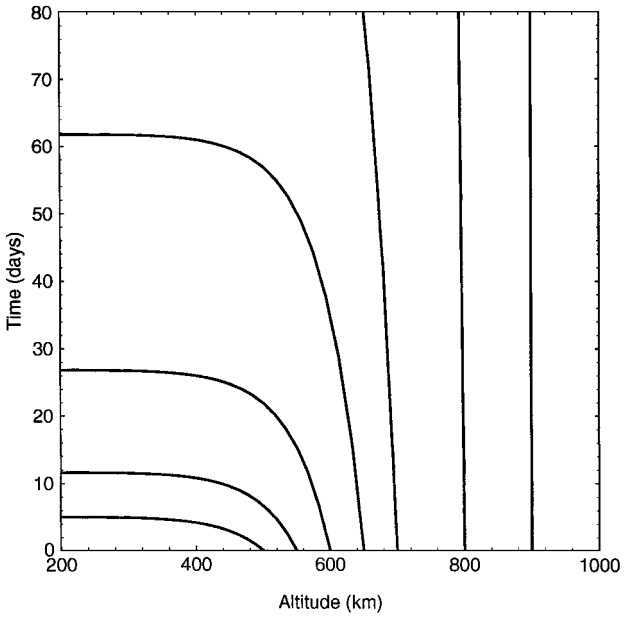

Fig. 5 Family of characteristics for nanosatellites with a ballistic coefficient of 20 kg m^{-2}.

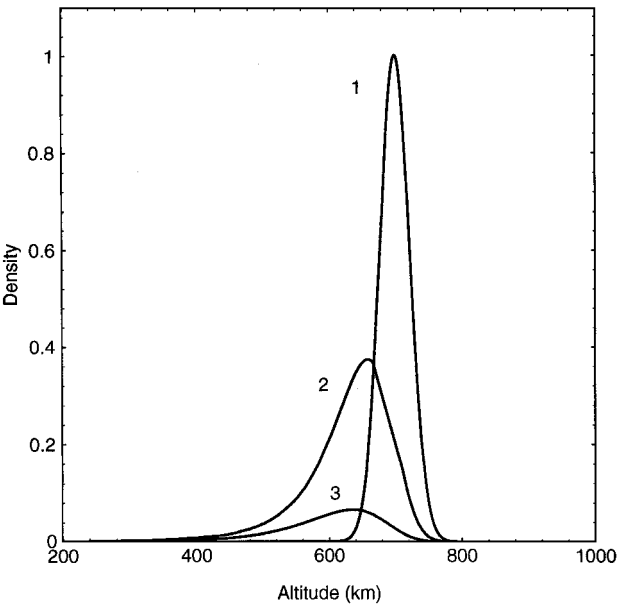

Fig. 6a Evolution of a narrow Gaussian distribution of nanosatellites in a planar constellation: 1, t = 0 days; 2, t = 100 days; and 3, t = 200 days.

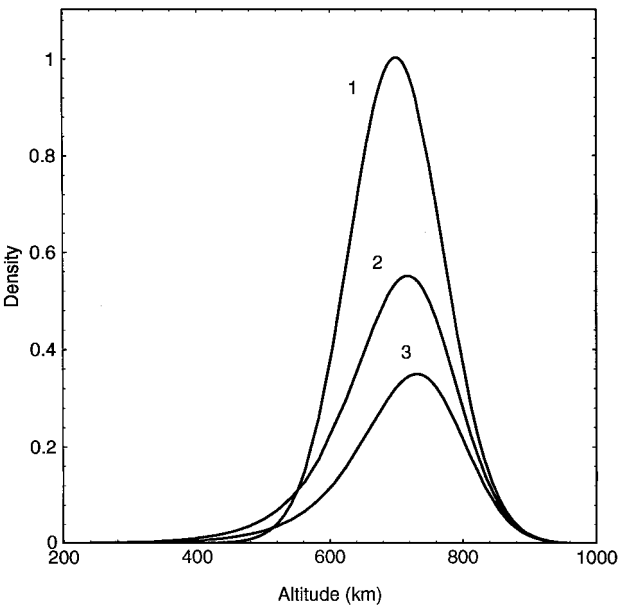

Fig. 6b Evolution of a broad Gaussian distribution of nanosatellites in a planar constellation: 1, t = 0 days; 2, t = 100 days; and 3, t = 200 days.

distribution of nanosatellites under the action of air drag only. This is of direct relevance for some mission applications.[5] Then, Eq. (9b) becomes

$$\frac{\mathrm{d}n(r,t)}{\mathrm{d}r} + n(r,t)\left[\frac{v_r'(r)}{v_r(r)} + \frac{1}{r}\right] = 0 \tag{14}$$

which can be solved directly to obtain the free decay of the constellation as

$$\ln\{n(r,t)\} = \ln\{rv_r(r)\}^{-1} + \Psi[G(r,t)] \tag{15}$$

Because we are ultimately solving a partial differential equation, the term $\Psi[G(r,t)]$ is an arbitrary function of the characteristic equation that must be now determined from the initial distribution of nanosatellites $n(r,0)$. For illustration, the nanosatellite constellation will now be modeled using a Gaussian distribution of mean number density with orbit radius. This will be used to represent the distribution of nanosatellites after they have dispersed in azimuth into a uniform thin disk, as discussed in Sec. II. Therefore, the initial number density of the distribution will be written as

$$n(r,0) = n_m \exp\left[-\lambda(r - r_m)^2\right] \tag{16}$$

where the parameters n_m and λ describe the shape of the initial distribution with the peak density occurring at orbit radius r_m. Although this functional form has been chosen for illustration, other initial distributions can, of course, be considered. From Eq. (15), the unknown function Ψ may now be obtained from $n(r,0)$, the initial data for the solution at $t = 0$, as

$$\Psi(z) = \ln\left\{n_m \exp\left[-\lambda(H\ln z - r_m)^2\right]\right\} - \ln\left\{-\varepsilon z^{-1}(H\ln z)^{\frac{3}{2}}\right\} \tag{17}$$

with independent variable $z = G(r,0) = \exp(r/H)$. The solution of the evolution equation for this initial Gaussian distribution then becomes

$$\ln\left\{n(r,t)\right\} = \ln\left\{-\varepsilon r^{\frac{3}{2}}\exp[-r/H]\right\}^{-1} + \Psi\left\{\exp[r/H] + (\varepsilon\sqrt{r}/H)t\right\} \tag{18}$$

The solution shown in Fig. 6a illustrates the evolution of an initially narrow Gaussian distribution of nanosatellites centred at an altitude of 700 km. The parameter n_m has been taken to be unity so that the solutions are nondimensional. It can be seen that the width of the distribution increases as the shearing motion due to the differential air drag acts on the constellation. Moreover, due to the broadening of the distribution, the peak number density rapidly falls. For a wider initial distribution, however, the nanosatellites at low altitude decay faster than the distribution can be replenished from above. The altitude of peak density then moves outward through the distribution, as shown in Fig. 6b. Therefore, under certain conditions the peak density of the constellation in fact moves to higher altitudes and not, as expected, to lower altitudes.

VI. Evolution Equation for a Spherical Constellation

The evolution of a spherical constellation of nanosatellites can also be obtained using the methods already described. In this case the nanosatellites will be dispersed in both azimuth and inclination and ascending node to provide a spherically symmetric constellation. By considering the continuity of nanosatellites in a spherical shell of thickness Δr, an evolution equation can again be obtained. In this case a shell of the constellation bounded by the interval $[r, r + \Delta r]$ will contain $4\pi r^2 \Delta r n(r,t)$ nanosatellites. Using the

continuity arguments of Sec. III, the evolution equation is found to be

$$\frac{\partial n(r,t)}{\partial t} + \frac{1}{r^2}\frac{\partial}{\partial r}\left[r^2 v_r(r) n(r,t)\right] = \dot{n}^+(r) - \dot{n}^-(r) \tag{19}$$

Again, this partial differential equation may be separated into two ordinary differential equations representing the characteristics of the problem and the evolution of the mean number density of nanosatellites, namely,

$$\frac{\mathrm{d}r}{\mathrm{d}t} = v_r(r) \tag{20a}$$

$$\frac{\mathrm{d}n(r,t)}{\mathrm{d}r} + n(r,t)\left[\frac{2}{r} + \frac{v_r'(r)}{v_r(r)}\right] = \frac{1}{v_r(r)}\left[\dot{n}^+(r) - \dot{n}^-(r)\right] \tag{20b}$$

The characteristic equation for the spherical constellation is identical to that of the planar case, defined by Eq. (13). Therefore, solutions to Eq. (20b) represent the evolution of the mean number density of nanosatellites under the action of air drag and various models for the forcing terms $\dot{n}^+(r, t)$ and $\dot{n}^-(r, t)$.

VII. Solution of the Evolution Equation for a Spherical Constellation

Free Evolution

If the forcing terms $\dot{n}^+(r, t)$ and $\dot{n}^-(r, t)$ are removed from Eq. (20b), standard solution methods provide the mean number density of nanosatellites under the action of air drag alone as

$$\ell n\{n(r,t)\} = \ell n\left\{r^2 v_r(r)\right\}^{-1} + \Psi[G(r,t)] \tag{21}$$

where $\Psi[G(r, t)]$ is again an arbitrary function of the characteristic equation that must be obtained from the initial distribution of nanosatellites $n(r, 0)$ to satisfy the boundary conditions of the Cauchy problem. For illustration, the nanosatellite constellation will now be modeled using a modified Gaussian distribution of nanosatellite number density. Again, this represents the distribution of nanosatellites after they have been uniformly dispersed. The initial number density of the distribution will now be defined as

$$n(r,0) = n_m \exp\left[-\lambda(r - r_m)^{\kappa}\right] \tag{22}$$

where the parameter κ shapes the profile of the initial distribution, with large values of κ generating a flat distribution. Again, this functional form is used for illustration. Other initial distributions can of course be considered. The solution shown in Fig. 7 illustrates the evolution of a broad, flat distribution ($\kappa = 6$) centred at an altitude of 700 km. Again, the parameter n_m has been taken to be unity so that the solutions are nondimensional. It can be seen that the width of the distribution decreases as the shearing motion due to differential air drag acts on the constellation. For this wide initial distribution, the nanosatellites at low altitudes decay faster than the distribution can be replenished from above. The altitude of peak density then moves outward, leaving a persistent high altitude Gaussian-type distribution.

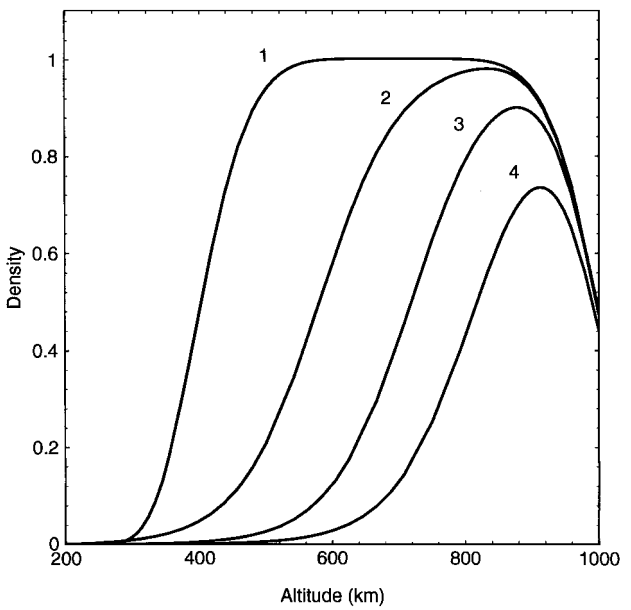

Fig. 7 Evolution of a flat distribution of nanosatellites in a spherical constellation: 1, t = 0 days; 2, t = 20 days; 3, t = 200 days; and 4, t = 1000 days.

Forced Evolution

The preceding analysis has considered the evolution of an initial distribution of nanosatellites under the action of air drag only. To extend the analysis, functions will be added to describe the deposition of new nanosatellites into the distribution and the on-orbit failure of existing nanosatellites. Whereas the characteristic equation remains unchanged, a new evolution equation must now be solved. Retaining the forcing terms, it can be seen that Eq. (20b) has an integrating factor $r v_r(r)$ and so can be written as

$$\frac{\mathrm{d}}{\mathrm{d}r}\left[n(r,t) r^2 v_r(r)\right] = r^2\left[\dot{n}^+(r) - \dot{n}^-(r)\right] \tag{23}$$

If the forcing terms are time independent, Eq. (23) then integrates directly to

$$n(r,t) = \frac{1}{r^2 v_r(r)}\int r^2\left[\dot{n}^+(r) - \dot{n}^-(r)\right]\mathrm{d}r + \Psi[G(r,t)] \tag{24}$$

Then, by the substitution of appropriate functions for $\dot{n}^+(r)$ and $\dot{n}^-(r)$ in Eq. (24), the long-term evolution of the nanosatellite constellation can be investigated. Whereas $\dot{n}^-(r, t)$ can be used to describe the removal or failure of nanosatellites, truly random failure requires a somewhat more complex analysis.

Evolution with On-Orbit Failures

In any large constellation of nanosatellites, on-orbit failure will have implications for the long-term viability of the system. In general, such failures are likely to be random uncorrelated events, so that the mean failure rate is directly proportional to the number density of nanosatellites. Therefore, if the nanosatellites have a fixed mean failure rate of η, the rate of removal of active satellites $\dot{n}^-(r, t)$ becomes

$$\dot{n}^-(r,t) = -\eta n(r,t) \tag{25}$$

which is time dependant, even for a constant mean failure rate. By the assumption that there is no deposition of new nanosatellites, the term $\dot{n}^+(r)$ can be removed and so the evolution equation now becomes

$$\frac{\mathrm{d}n(r,t)}{\mathrm{d}r} + n(r,t)\left[\frac{2}{r} + \frac{v_r'(r)}{v_r(r)} + \frac{\eta}{v_r(r)}\right] = 0 \tag{26}$$

Again, standard solution methods yield the mean number density of nanosatellites with a constant mean failure rate as

$$\ell n\{n(r,t)\} = \ell n\left\{r^2 v_r(r)\right\}^{-1} + (\eta H / \varepsilon\sqrt{R})\exp[r/H] + \Psi[G(r,t)] \tag{27}$$

The initial distribution defined by Eq. (22) will again be used to illustrate the effect of random failures. The evolution of the constellation with a mean failure rate of 10^{-8} s^{-1} (corresponding to a mean nanosatellite lifetime of 3.17 years) is shown in Fig. 8. It can be seen that the constellation decays as before due to air drag, with on-orbit failures reducing the overall number density of nanosatellites. Because the removal rate is proportional to the nanosatellite number density, on-orbit failure is of little consequence to those members of the constellation at low altitudes that have a short life due to air drag.

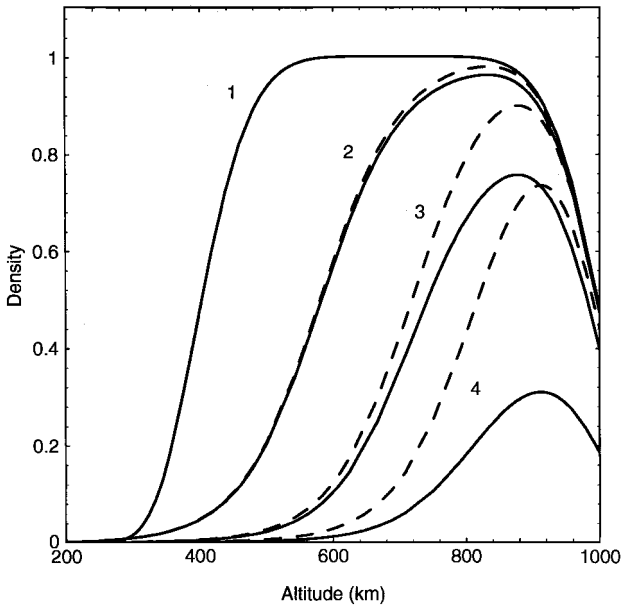

Fig. 8 Evolution of a flat distribution of nanosatellites with random on-orbit failures: 1, $t = 0$ days; 2, $t = 20$ days; 3, $t = 200$ days; 4, $t = 1000$ days; ——, failures; and – – –, no failures.

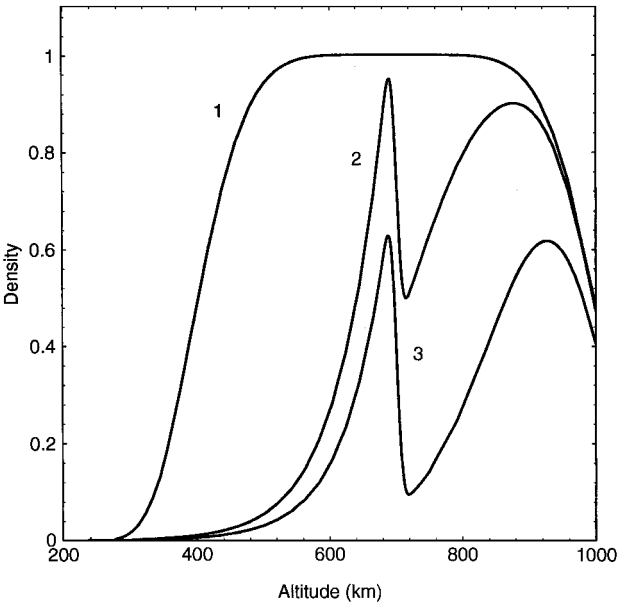

Fig. 9 Evolution of a flat distribution of nanosatellites with deposition: 1, $t = 0$ days; 2, $t = 200$ days; and 3, $t = 2000$ days.

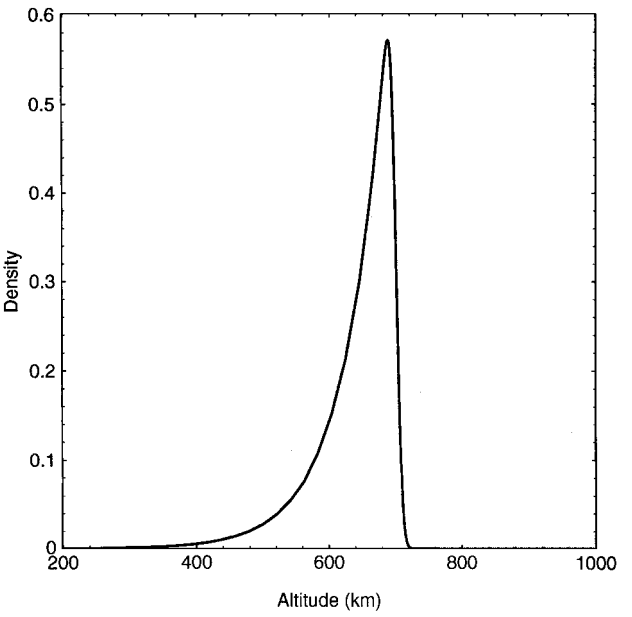

Fig. 10 Asymptotic distribution of nanosatellites.

Evolution with Deposition of New Nanosatellites

Whereas on-orbit failure can be a relatively minor effect compared to differential air drag, the deposition of new nanosatellites will have a major effect on the population dynamics of the constellation. It has been seen that differential air drag quickly removes nanosatellites from low orbits so that the deposition of new nanosatellites may be required to maintain a uniform constellation. This is of particular importance for schemes with nanosatellites that have no active propulsion.[5] It will be assumed that the long-term, mean deposition rate is time independent, with nanosatellites being dispensed as discussed in Sec. II and that the deposition is centered on some particular orbit radius. Then, for illustration, the evolution of the constellation will now be considered with a Gaussian deposition function of the form

$$\dot{n}^+(r) = \dot{n}_m \exp\left[-\gamma(r - r_d)^2\right] \tag{28}$$

where the deposition of new nanosatellites is centered at orbit radius r_d. Other functional forms for $\dot{n}^+(r)$ can of course be considered. By assuming that the terms $\dot{n}^-(r)$ can be ignored, Eq. (24) provides the mean number density of nanosatellites as

$$n(r,t) = \frac{\dot{n}_m}{r^2 v_r(r)}\left[\frac{\sqrt{\pi}}{4\gamma^{\frac{3}{2}}}(1 + 2\gamma r_d^2)\operatorname{erf}\left[\sqrt{\gamma}(r - r_d)\right] - \frac{(r + r_d)}{2\gamma}\exp\left[-\gamma(r - r_d)^2\right]\right] + \frac{1}{r^2 v_r(r)}\Psi[G(r,t)] \tag{29}$$

The evolution of the initial flat distribution defined by Eq. (22) is shown in Fig. 9 with the deposition of new nanosatellites centered at an altitude of 700 km with a mean deposition rate of 2×10^{-7} s^{-1}. It can be seen that, while the deposition of new nanosatellites replenishes the distribution in the vicinity of orbit radius r_d, the constellation still decays under the action of air drag. Deposition of new nanosatellites in this way is therefore unable to maintain a uniform distribution due to the rapid shearing of nanosatellites in low orbits by differential air drag. The asymptotic limit of the distribution as $t \to \infty$ can now be obtained to assess the steady-state distribution of the constellation.

Asymptotic Distribution

The steady-state distribution of nanosatellites under the action of deposition and air drag can be obtained by setting $\partial n(r,t)/\partial t = 0$. Then, Eq. (19) provides the steady-state distribution of nanosatellites $n_\infty(r)$ for some deposition function $\dot{n}^+(r)$ as

$$n_\infty(r) = \frac{1}{r^2 v_r(r)}\int r^2 \dot{n}^+(r)\,\mathrm{d}r + D \tag{30}$$

where D is a constant of integration. The steady-state distribution for the deposition function discussed earlier is shown in Fig. 10. It can be seen that in the limit as $t \to \infty$ a persistent Gaussian-type distribution remains, centered at orbit radius r_d. Rather than propose deposition functions $\dot{n}^+(r)$ and calculate the steady-state distribution of nanosatellites, Eq. (19) can be used to solve the inverse problem.

The inverse problem is posed by finding the mean deposition rate required to obtain some desired steady-state distribution of nanosatellites $n_\infty(r)$. Ignoring on-orbit failures and applying the steady-state condition to Eq. (19) yields

$$\dot{n}^+(r) = \frac{1}{r^2}\frac{\partial}{\partial r}\left[r^2 v_r(r) n_\infty(r)\right] \tag{31}$$

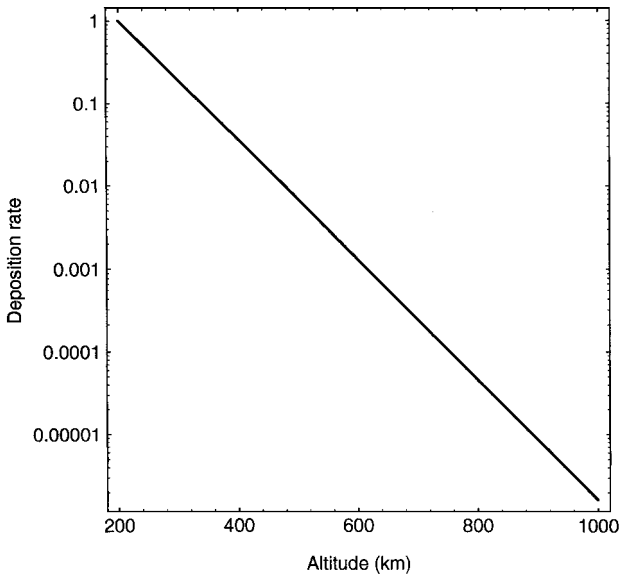

Fig. 11 Required deposition rate for a uniform steady-state distribution.

For example, if a uniform distribution of nanosatellites is required, such that $n_\infty(r) = n_*$ is constant, the mean deposition rate is obtained from Eq. (31) as

$$\dot{n}^+(r) = (\varepsilon\sqrt{R}n_*/2r)[r/2H - 1]\exp[-r/H] \qquad (32)$$

The functional form of this deposition profile is shown in Fig. 11, nondimensionalizing the deposition rate relative to that required at an altitude of 200 km. It can be seen that rapid deposition is required at low altitudes to replenish the constellation because the transport of nanosatellites to lower orbits by differential air drag is insufficient to maintain a uniform distribution. If a uniform distribution is only required at higher altitudes, then a much more modest mean deposition rate is required. However, Eq. (32) demonstrates that the deposition of new nanosatellites must be biased toward lower altitudes if a uniform distribution is required, as expected.

VIII. Conclusions

A simple analytical model has been developed to investigate the long-term evolution of nanosatellite constellations under the action of air drag, on-orbit satellite failures, and the deposition of new satellites into the constellation. It has been shown that, due to the shearing effect of differential drag, an initially compact constellation broadens, as expected. However, under certain conditions, it has been found that the peak nanosatellite number density, in fact, moves outward, through the constellation. With a mean deposition function added to represent the addition of new nanosatellites to the constellation, the long-term evolution of the entire constellation can be investigated. Finally, asymptotic methods allow the steady-state distribution of nanosatellites to be evaluated. Given some required steady-state distribution, an inverse approach allows the required deposition rate of new nanosatellite to be determined.

References

[1] Janson, S. W., "Mini-, Micro-, and Nanosatellite Concepts," *Micro and Nanotechnology for Space Systems: An Initial Evaluation*, Monograph 97-01, The Aerospace Press, El Segundo, CA, and AIAA, Reston, VA, 1993, pp. 41–45.

[2] Salvo, C. G., "Advanced Space Technology X2000," *Proceedings of the 3rd International Academy of Astronautics International Conference on Low Cost Planetary Missions*, Paper L98-0402, April–May 1998.

[3] Janson, S. W., "Silicon Satellites: Picosats, Nanosats and Microsats," *Proceedings of the International Conference on Integrated Micro/Nanotechnology for Space Applications*, The Aerospace Press, El Segundo, CA, and AIAA, Reston, VA, 1995.

[4] Burch, J. L., "Toward a Sun–Earth Connection Strategic Plan for 2000-2010," American Geophysical Union Spring Meeting, Baltimore, MD, May 1996.

[5] Elliot, C. J., "World-Wide 'Instantaneous' Messaging—The Telex Users' Iridium," *Symposium on Systems and Services for Small Satellites*, Arcachon, France, June 1992.

[6] Fleeter, R., "Design of Low-Cost Spacecraft," *Space Mission Analysis and Design*, edited by J. R. Wertz and W. J. Larson, Kluwer Academic, Dordrecht, The Netherlands, 1991, pp. 711–738.

[7] McInnes, C. R., "An Analytical Model for the Catastrophic Production of Orbital Debris," *ESA Journal*, Vol. 17, No. 4, 1993, pp. 293–305.

[8] Murphy, I. S., *Advanced Calculus*, Arklay Stirling, UK, 1984, pp. 79–101.

[9] Pisacane, V. L., and Moore, R. G. (eds.), *Fundamentals of Space Systems*, Oxford Univ. Press, New York, 1994, pp. 48–54.